

AD-A144594

AFWAL-TR-84-2036

LIBRARY
RESEARCH REPORTS DIVISION
NAVAL POSTGRADUATE SCHOOL
MONTEREY, CALIFORNIA 93943



DEVELOPMENT OF A DESIGN-ORIENTED NAVIER-STOKES
CASCADE ANALYSIS

S. J. Shamroth
H. McDonald

SCIENTIFIC RESEARCH ASSOCIATES, INC.
P O BOX 498
GLASTONBURY, CONNECTICUT 06033

910006 F

JUNE 1984

FINAL REPORT FOR PERIOD SEPTEMBER 1983 - MARCH 1984

APPROVED FOR PUBLIC RELEASE; DISTRIBUTION UNLIMITED.

AERO PROPULSION LABORATORY
AIR FORCE WRIGHT AERONAUTICAL LABORATORIES
AIR FORCE SYSTEMS COMMAND
WRIGHT-PATTERSON AIR FORCE BASE, OHIO 45433

NOTICE

When Government drawings, specifications, or other data are used for any purpose other than in connection with a definitely related Government procurement operation, the United States Government thereby incurs no responsibility nor any obligation whatsoever; and the fact that the government may have formulated, furnished, or in any way supplied the said drawings, specifications, or other data, is not to be regarded by implication or otherwise as in any manner licensing the holder or any other person or corporation, or conveying any rights or permission to manufacture use, or sell any patented invention that may in any way be related thereto.

This report has been reviewed by the Office of Public Affairs (ASD/PA) and is releasable to the National Technical Information Service (NTIS). At NTIS, it will be available to the general public, including foreign nations.

This technical report has been reviewed and is approved for publication.



MARVIN A. STIBICH

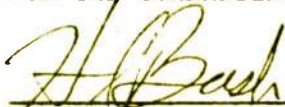
TAM, Compressor Research Group



WALKER H. MITCHELL

Chief, Technology Branch

FOR THE COMMANDER



H. IVAN BUSH

Director, Turbine Engine Division

"If your address has changed, if you wish to be removed from our mailing list, or if the addressee is no longer employed by your organization please notify AFWAL/POTX, W-PAFB, OH 45433 to help us maintain a current mailing list".

Copies of this report should not be returned unless return is required by security considerations, contractual obligations, or notice on a specific document.

UNCLASSIFIED

SECURITY CLASSIFICATION OF THIS PAGE (When Data Entered)

REPORT DOCUMENTATION PAGE		READ INSTRUCTIONS BEFORE COMPLETING FORM
1. REPORT NUMBER AFWAL-TR-84-2036	2. GOVT ACCESSION NO.	3. RECIPIENT'S CATALOG NUMBER
4. TITLE (and Subtitle) DEVELOPMENT OF A DESIGN-ORIENTED NAVIER-STOKES CASCADE ANALYSIS		5. TYPE OF REPORT & PERIOD COVERED Final Report September 1983-March 1984
		6. PERFORMING ORG. REPORT NUMBER 910006F
7. AUTHOR(s) S.J. Shamroth H. McDonald		8. CONTRACT OR GRANT NUMBER(s) F33615-83-C-2370
9. PERFORMING ORGANIZATION NAME AND ADDRESS Scientific Research Associates, Inc. P.O. Box 498 Glastonbury, CT 06033		10. PROGRAM ELEMENT, PROJECT, TASK AREA & WORK UNIT NUMBERS P.E. 65502F Task 300520 Work Unit 30052005
11. CONTROLLING OFFICE NAME AND ADDRESS Aero Propulsion Laboratory (AFWAL/POTX) Air Force Wright Aeronautical Laboratories (AFSC) Wright-Patterson Air Force Base, Ohio 45433		12. REPORT DATE June 1984
14. MONITORING AGENCY NAME & ADDRESS (If different from Controlling Office)		13. NUMBER OF PAGES 43
		15. SECURITY CLASS. (of this report) Unclassified
15a. DECLASSIFICATION/DOWNGRADING SCHEDULE		
16. DISTRIBUTION STATEMENT (of this Report) Approved for public release; distribution unlimited.		
17. DISTRIBUTION STATEMENT (of the abstract entered in Block 20, if different from Report)		
18. SUPPLEMENTARY NOTES		
19. KEY WORDS (Continue on reverse side if necessary and identify by block number)		
20. ABSTRACT (Continue on reverse side if necessary and identify by block number) Under a Phase I SBIR effort, an existing Navier-Stokes cascade computer code has been automated and recoded to form a design-oriented cascade calculation procedure. The procedure consists of two distinct codes which are (1) the coordinate generation code and (2) the Navier-Stokes solver. With the revised procedure, the coordinate generator allows a new user to obtain suitable coordinate systems with a minimum of input data. The Navier-Stokes procedure has been recoded to minimize required input and to decrease run time per time step. In addition, a		

UNCLASSIFIED

SECURITY CLASSIFICATION OF THIS PAGE (When Data Entered)

run protocol has been developed to obtain rapid convergence. A demonstration calculation has been run which yields a converged solution in less than 300 CPU secs of unvectorized CRAY-1 run time.

UNCLASSIFIED

SECURITY CLASSIFICATION OF THIS PAGE (When Data Entered)

TABLE OF CONTENTS

	Page
INTRODUCTION	1
ANALYSIS	4
Governing Equations	4
Numerical Procedures	5
Artificial Dissipation	6
Boundary Conditions	8
Turbulence Models	10
CURRENT EFFORTS	13
Objective	13
Coordinate System	13
Navier-Stokes Analysis	19
ESTIMATES OF TECHNICAL FEASIBILITY	22
REFERENCES	24
FIGURES.	27
APPENDIX A	39

INTRODUCTION

Although the two-dimensional cascade analysis represents a simplified version of the actual three-dimensional flow field which includes end wall effects, the two-dimensional problem gives significant insight into the cascade flow field and obviously is a necessary first step in developing a three-dimensional analysis. Hence, cascade analyses of various types have been a subject of high interest in recent years. Among the analyses being pursued are inviscid analyses (e.g. Refs. 1 and 2), inviscid analyses with boundary layer corrections (e.g. Ref. 3) and Navier-Stokes analyses (e.g. Ref. 4 and 5). Each of these approaches are viable under certain circumstances. Inviscid analyses can give good predictions of the blade pressure distribution for conditions where the effect of viscous phenomena upon the blade pressure distribution remains small. However, inviscid analyses require some method of assuming airfoil circulation to obtain a unique flow solution. In general this specification is straight-forward for sharp trailing edged blades in steady flow where the Kutta-Joukowski condition serves to specify circulation. However, in cases where the trailing edge is rounded or the flow is unsteady or trailing edge separation occurs, specification of a proper condition is ambiguous. In addition since inviscid methods are devoid of viscous effects by definition, they obviously cannot give either heat transfer or viscous loss information.

If an inviscid analysis is combined with a boundary layer analysis in either a strong interaction or weak interaction mode, some of these limitations may be relieved. In cases where the viscous displacement effect has an insignificant or only small effect on the actual blade pressure distribution, an inviscid calculation can be used to obtain the pressure distribution and a boundary layer calculation then made to obtain heat transfer and loss effects. However, in many cases such as when boundary layers thicken significantly or separate, the viscous displacement effect may alter the pressure distribution. This may be a particular problem in transonic flow where the local pressure distribution and shock location become very sensitive to small change in the effective passage area. In these cases a strong interaction solution is required to account for the mutual effects of the viscous boundary layer and the nominally inviscid core flow.

A strong interaction analysis may take the form of either a forward marching procedure or a global iteration. For regions where the outer nominally inviscid flow is supersonic (and thus described by hyperbolic equations) a solution can be spatially forward marched in the nominally streamwise direction with the inviscid and viscous regions coupled on a station-by-station basis. Obviously, the analysis is limited by the governing assumptions which include lack of viscous effects in the outer region and neglect of normal pressure gradients and streamwise diffusion in the inner region. The chief numerical difficulty with this approach is the stiff nature of the coupled sets of equations which is manifested in the appearance of physically unrealistic branching solutions. In regions where the outer flow is subsonic, the outer flow equations are elliptic in nature and in these regions forward marching in the streamwise spatial direction is not possible and consequently a series of viscous and inviscid calculations must be performed in which each corrects the other in a global manner.

Problems with interaction solutions become particularly severe in transonic flows where both subsonic and supersonic nominally inviscid regions are present and where small viscous displacement effects may have a major effect on the blade pressure distribution and shock location. A final difficulty with the interactive approach occurs when boundary layer separation appears. Here with an imposed pressure field, the usual steady state boundary layer equations are unstable when solved as an initial value problem in space in regions of reversed flow. However, the equations can be marched in space by suppressing the streamwise convection term in the separated region (Ref. 6). Although this approximation allows the solution to be marched through separation, the approximation becomes progressively more inaccurate as the extent of the separation zone or the magnitude of either the normal or the back flow velocities become large. Thus, calculated flow details which may be important (such as heat transfer at reattachment) may have significant error when separation is present and such an interactive analysis is used. Other schemes have and are being developed which solve the interaction problem without encountering an instability by either changing the problem to initial value in time or iteration space. Nonetheless the resulting solutions still retain the approximations of the boundary layer equations and the inviscid flow. However, as with inviscid flow solutions,

combined viscous and inviscid solutions remain a valuable tool for those classes of cascade problems where the approximations adopted are valid.

The final procedure currently available is the solution of full ensemble-averaged Navier-Stokes equations. Such an analysis has been applied to a variety of cascade flow fields by Shamroth, Gibeling and McDonald (Ref. 7), Shamroth, McDonald and Briley (Refs. 5, 8-10) and by Shamroth and McDonald (Ref. 4). The use of the full Navier-Stokes equations for the cascade problem allows use of a single set of equations for the entire flow field and thus removes the need for an interaction analysis to couple different equation descriptions for different flow regions. The analysis simultaneously predicts both the blade pressure distribution and viscous and heat transfer effects.

To date this Navier-Stokes analysis has been tested against a variety of sets of cascade experimental data. These include the turbine cascades of Turner (Ref. 11) and Hylton, Mihelc, Turner, Nealy and York (Ref. 12), the compressor cascades of Stephens and Hobbs (Ref. 13) and Hobbs, Wagner, Dannenhoffer and Dring (Ref. 14) and the compressor rotor cascade of Dring, Joslyn and Harden (Ref. 15). Since most experimental data is limited to surface pressure data, the comparisons made are primarily between calculated and measured surface pressure distributions. However, in Ref. 16 comparisons are made between predicted and measured surface heat transfer rates and Ref. 17 gives velocity profile comparisons. In general, the comparisons are quite favorable and indicate the Navier-Stokes approach to be a viable and practical technique for predicting cascade flow fields which does not contain the possible inadequacies of more approximate approaches. Details of the results are given in the cited references.

Although these results show the Navier-Stokes approach to hold considerable promise as a design tool, at the initiation of the current effort the code required user expertise to obtain an accurate, converged solution in an efficient manner. The purpose of the present effort was to revise the code so as to allow a user with little prior experience to utilize the procedure in an effective manner. The changes made to reach this objective are discussed in the present report. However, prior to a discussion of these changes a brief review of the analysis is given.

II. ANALYSIS

The present analysis is based upon a solution of the ensemble-averaged Navier-Stokes equations using the linearized block implicit (LBI) method of Briley and McDonald (Ref. 18). The equations are solved in a constructive coordinate system (Ref. 4) with density and the Cartesian velocity components being taken as dependent variables. The application of the LBI method to the cascade flow field problem has been discussed in some detail in Refs. 4, and 7-10. However, for completeness it will be repeated here along with a brief discussion of the coordinate system and governing equations.

Governing Equations

The present effort solves the time-dependent compressible Navier-Stokes equations to predict the cascade flow field. If the computational spatial coordinates are ξ and η where

$$\xi = \bar{\xi}(x, y, t) \quad \eta = \eta(x, y, t) \quad \tau = t \quad (1)$$

then the continuity equation, the x-component of the momentum equation and the y-component of the momentum equation are written as

$$\begin{aligned} \frac{\partial W}{\partial \tau} + \xi_t \frac{\partial W}{\partial \xi} + \xi_x \frac{\partial F}{\partial \xi} + \xi_y \frac{\partial G}{\partial \xi} + \eta_t \frac{\partial W}{\partial \eta} + \eta_x \frac{\partial F}{\partial \eta} + \eta_y \frac{\partial G}{\partial \eta} \\ = \frac{1}{Re} \left[\xi_x \frac{\partial F_1}{\partial \xi} + \eta_x \frac{\partial F_1}{\partial \eta} + \xi_y \frac{\partial G_1}{\partial \xi} + \eta_y \frac{\partial G_1}{\partial \eta} \right] \end{aligned} \quad (2)$$

where

$$W = \begin{pmatrix} \rho \\ \rho u \\ \rho v \end{pmatrix}, \quad F = \begin{pmatrix} \rho u \\ \rho u^2 + p \\ \rho uv \end{pmatrix}, \quad G = \begin{pmatrix} \rho v \\ \rho uv \\ \rho v^2 + p \end{pmatrix}, \quad F_1 = \begin{pmatrix} 0 \\ \tau_{xx} \\ \tau_{xy} \end{pmatrix}, \quad G_1 = \begin{pmatrix} 0 \\ \tau_{xy} \\ \tau_{yy} \end{pmatrix} \quad (3)$$

In Eqs. (1-3) x and y are Cartesian coordinates, t is time, u and v are velocity components, ρ is density, p is pressure, and τ_{ij} is the stress tensor and Re is the Reynolds number.

The dependent variables chosen for the present formulation are the density, ρ , and the velocity components, u and w . Although the code does contain an energy equation and calculations have been made with an energy equation, most calculations have been run with the assumption T^0 , the stagnation temperature, equals a constant. With this assumption, the pressure is related to the velocity and density by

$$P = \rho R \left(T^0 - \frac{(u^2 + v^2)}{2C_p} \right) \quad (4)$$

This approximation of constant stagnation temperature has been made solely to conserve run time. Calculations made with an energy equation (e.g. Ref. 16) have shown no problems in converging and have given surface pressure and heat transfer distributions in good agreement with data. However, inclusion of the energy equation obviously requires additional computer run time.

Numerical Procedure

The numerical procedure used to solve the governing equations is a consistently split linearized block implicit (LBI) scheme originally developed by Briley and McDonald (Ref. 18). A conceptually similar scheme has been developed for two-dimensional MHD problems by Lindemuth and Killeen (Ref. 19). The procedure is discussed in detail in Refs. 18 and 20. The method can be briefly outlined as follows: the governing equations are replaced by an implicit time difference approximation, optionally a backward difference or Crank-Nicolson scheme. Terms involving nonlinearities at the implicit time level are linearized by Taylor expansion in time about the solution at the known time level, and spatial difference approximations are introduced. The result is a system of multi-dimensional coupled (but linear) difference equations for the dependent variables at the unknown or implicit time level. To solve these difference equations, the Douglas-Gunn (Ref. 21) procedure for generating alternating-direction implicit (ADI) schemes as perturbations of fundamental implicit difference schemes is introduced in its

natural extension to systems of partial differential equations. This technique leads to systems of coupled linear difference equations having narrow block-banded matrix structures which can be solved efficiently by standard block-elimination methods.

The method centers around the use of a formal linearization technique adapted for the integration of initial-value problems. The linearization technique, which requires an implicit solution procedure, permits the solution of coupled nonlinear equations in one space dimension (to the requisite degree of accuracy) by a one-step noniterative scheme. Since no iteration is required to compute the solution for a single time step, and since only moderate effort is required for solution of the implicit difference equations, the method is computationally efficient; this efficiency is retained for multi-dimensional problems by using what might be termed block ADI techniques. The method is also economical in terms of computer storage, in its present form requiring only two time-levels of storage for each dependent variable. Furthermore, the block ADI technique reduces multi-dimensional problems to sequences of calculations which are one-dimensional in the sense that easily-solved narrow block-banded matrices associated with one-dimensional rows of grid points are produced. A more detailed discussion of the solution procedure as discussed by Briley, Buggeln and McDonald (Ref. 22) is given in the Appendix A.

Artificial Dissipation

Since the calculations of interest are often at high Reynolds numbers typical of normal turbomachinery applications, it is necessary to add "artificial dissipation" terms to suppress spatial oscillations associated with central spatial differences approximations. This can be done via a dissipative spatial difference formulation (e.g., one-sided difference approximations for first derivatives) or by explicitly adding an additional dissipative type term. For the Navier-Stokes equations, the present authors favor the latter approach since when an additional term is explicitly added, the physical approximation being made is usually clearer than when dissipative mechanisms are contained within numerical truncation errors, and further, explicit addition of an artificial dissipation term allows greater control over the amount of non-physical dissipation being added.

Obviously, the most desirable technique would add only enough dissipative mechanism to suppress oscillations without deteriorating solution accuracy. Various methods of adding artificial dissipation were investigated in Ref. 8, and these were evaluated in the context of a model one-dimensional problem containing a shock with a known analytic solution (one-dimensional flow with heat transfer). The methods which were considered included second-order dissipation, fourth-order dissipation and pressure dissipation techniques.

As a result of this investigation, it was concluded that a second-order anisotropic artificial dissipation formulation suppressed spatial oscillations without impacting adversely on accuracy and could be used to capture the nearly normal shocks which are expected in transonic cascades successfully. In this formulation the terms

$$\frac{\partial}{\partial x} \left(d_x \frac{\partial \phi}{\partial x} \right) \quad \frac{\partial}{\partial y} \left(d_y \frac{\partial \phi}{\partial y} \right)$$

are added to the governing equations where $\phi = u, v$ and ρ for the x-momentum, y-momentum and continuity equations, respectively. The exponent n is zero for the continuity equation and unity for the momentum equations. The dissipation coefficient d_x is determined as follows. The general equation has an x-direction convective term of the form $a \partial \phi / \partial x$ and an x-direction diffusion term of the form $\partial(b \partial \phi / \partial x) / \partial x$. The diffusive term is expanded

$$\partial(b \partial \phi / \partial x) / \partial x = b \partial^2 \phi / \partial x^2 + \partial b / \partial x \partial \phi / \partial x \quad (5)$$

and then a local cell Reynolds number $Re_{\Delta x}$ is defined for the x-direction by

$$Re_{\Delta x} = \left| a - \partial b / \partial x \right| \Delta x / b \quad (6)$$

where b is the total or effective viscosity including both laminar and turbulent contributions and Δx is the grid spacing. The dissipation coefficient d_x is non-negative and is chosen as the larger of zero and the local quantity $b (\sigma_x Re_{\Delta x} - 1)$. The dissipation parameter σ_x is a specified constant and represents the inverse of the cell Reynolds number below which no artificial dissipation is added. The dissipation coefficient

d_y is evaluated in an analogous manner and is based on the local cell Reynolds number $Re_{\Delta y}$ and grid spacing Δy for the y-direction and the specified parameter parameter σ_y .

The question arises as to the values of σ_x and σ_y which should be chosen. This was assessed both through the model problem (Ref. 8), and through calculations for a Jose Sanz compressor cascade (Refs. 4, 8 and 9). These results indicated that values of $\sigma = .5$ which corresponds to a cell Reynolds number 2 limitation would severely damp physical variations. However, when σ was set in the range $.025 \leq \sigma \leq 0.05$, which correspond to a cell Reynolds number range between 40 and 20, spurious spatial oscillations were damped with no significant change in the calculated results as σ was varied in this range. Further, as discussed in Refs. 4 and 7-10, the results obtained showed good agreement with data. This has since been confirmed at several other studies at Scientific Research Associates such as two- and three-dimensional transonic nozzle flows (Ref. 23) where a maximum acceptable value of $\sigma = 0.10$ has been noted for most problems. In some cases where spatial resolution may be marginal such as at the leading edge of a relatively sharp edged blade, it may be necessary to increase σ in this local area. However, σ can be decreased to 0.10 or below if computational grid points are added in this region.

Boundary Conditions

The authors' experience in solving Navier-Stokes equations has indicated the important role boundary conditions play in obtaining accurate solutions and rapid numerical convergence. Improper specification and/or implementation of boundary conditions can lead to adverse stability, convergence and accuracy properties for the solution procedure. In regard to specification of boundary conditions, the Navier-Stokes cascade analysis follows the suggestion of Briley and McDonald (Ref. 24) which specifies upstream total pressure and downstream static pressure conditions. For the cascade system shown in Fig. 1, AB and CD are periodic boundaries and periodic conditions are set here.

Specification of upstream and downstream conditions is somewhat more difficult. For an isolated cascade, boundary conditions for the differential equations may be known at both upstream infinity and downstream infinity.

However, since computation economics argues for placing grid points in the vicinity of the cascade and minimizing the number of grid points far from the cascade, the upstream and downstream computational boundaries should be set as close to the cascade as is practical. However, when the upstream boundary is placed close to the cascade, most flow function conditions on the boundary will not be known since these will have been changed from values at infinity by the presence of the cascade.

In the present approach, the suggestion of Ref. 24 is followed which sets total pressure on boundary BC (see Fig. 1). Unless boundary BC is very far upstream, the flow velocity along this boundary will not be equal to the velocity at upstream infinity since some inviscid deceleration will have occurred. However, as long as the boundary is upstream of the region of any significant viscous or shock phenomena, the total pressure on this boundary will be equal to the total pressure at upstream infinity. Hence, total pressure is an appropriate boundary condition realistically modeling the desired flow condition. In addition to specifying upstream total pressure, it is necessary to specify the inlet flow angle. In the present calculation, a value was assumed constant on the upstream boundary as a specified angle. The third condition set on the upstream boundary concerns the density and a zero density derivative at this boundary was specified as a numerical treatment of the boundary. The downstream boundary was treated by setting a constant static pressure as a boundary condition, and by setting second derivatives of both velocity components equal to zero at this location. In the present application, a constant static pressure was set at downstream infinity, and hence it is assumed that the downstream boundary is located in a region where pressure is uniform although a nonuniform specification is permitted. The final boundary conditions to be considered are the conditions along the blade surface. Here no-slip and no through-flow conditions were applied leading to a specification of zero velocity on the surface. An inviscid transverse momentum equation was applied on the surface leading to a boundary condition approximation of zero transverse pressure gradient being applied.

The second item which must be considered in regard to boundary conditions is their implementation. Both the upstream and downstream boundaries have boundary conditions associated with them which are nonlinear functions of the dependent variables. These are the specifications of total

pressure on the upstream boundary and static pressure on the downstream boundary. These nonlinear boundary conditions are linearized in the same manner as the governing equations, via a Taylor expansion of the dependent variables in time, and then solved implicitly along with the interior point equations. Although points on the periodic lines and the branch cut are boundaries to the computational regime, they are interior flow fields points and must be treated as such. The present technique replaces derivatives at these points by central differences. In addition, in regard to the periodic lines the procedure inverts a matrix with strict periodic boundary conditions; i.e., the periodic line values are obtained from the implicit solution, rather than from an extrapolation or averaging procedure which uses interior computational grid point values.

Turbulence Models

The existing cascade analysis contains three possible turbulence models. These are (i) a mixing length model, (ii) a turbulence energy-algebraic length scale model and (iii) a turbulence energy-turbulence dissipation model. In the mixing length model, the turbulent viscosity is related to the mean strain via a mixing length, ℓ , such that

$$\mu_T = \rho \ell \left[\left(\frac{\partial u_i}{\partial x_j} + \frac{\partial u_j}{\partial x_i} \right) \frac{\partial u_i}{\partial x_j} \right]^{1/2} \quad (7)$$

where μ_T is the turbulent viscosity, ρ is the density, ℓ is the mixing length, u_i is the i^{th} velocity component and x_i is the i^{th} Cartesian direction. Summation is implied for the repeated indices. The question now arises as to specification of ℓ . For the region upstream of the trailing edge, the mixing length is specified in the usual boundary layer manner; i.e.

$$\ell = \kappa_y (1 - e^{-y^+/27}) \quad \ell \leq \ell_{\max} \quad (8)$$

where κ is the von Karman constant and y^+ is the dimensionless normal coordinate, yu_T/ν . In boundary layer analysis ℓ_{\max} is usually taken as 0.09δ where δ is the boundary layer thickness taken as the location where $u/u_e = 0.99$. However, this definition of δ assumes the existence of an

outer flow where the velocity u_e is independent of distance from the wall at a given streamwise station; i.e., it assumes u_e is only a function of the streamwise coordinate. Although a boundary layer calculation will yield solutions in which u approaches u_e asymptotically at distances far from the solid no-slip surface, Navier-Stokes solutions for cascade flow fields do not in general predict a region where u asymptotes to a constant value. Furthermore, measurements of the flow also show no such region to exist in general. Obviously, a proper choice of δ for the Navier-Stokes cascade analysis is not straight forward. Calculations made in Refs. 4 and 7-9 have set the boundary layer thickness by first determining u_{\max} , the maximum streamwise velocity, at a given station and then setting δ via

$$\delta = 2.0y_{(u/u_{\max}=k)} \quad (9)$$

i.e., δ was taken as twice the distance for which $u/u_{\max} = k_1$. To date when k_1 has been taken as 0.80, this value has given reasonable results for several cases. In general, the boundary layer development including skin friction and heat transfer is sensitive to the choice of k_1 whereas the surface pressure distribution is relatively insensitive to this parameter.

The model used in the wake is also a mixing length model in which the mixing length was made proportional to the wake height, δ , and a linear growth of δ with distance was assumed based upon the classical free jet boundary results (Ref.25). With the free jet boundary growth assumption

$$\delta = (\delta_{ps} + \delta_{ss}) + (.2)(x - x_{TE}) \quad (10)$$

where δ_{ps} and δ_{ss} are the pressure and suction surface trailing edge boundary layer thickness and x_{te} is the trailing edge location. The mixing length, ℓ , was taken as 0.2δ . When using the mixing length model the user has the option of setting a transition location on suction and pressure surfaces. Most calculations run to date have been run with the mixing length model.

In addition to the mixing length model two alternate models are available. The first is based upon the usual partial differential equation for conservation of turbulence energy used in conjunction with an algebraic

length scale. The second is a turbulence energy-turbulence dissipation ($k-\epsilon$) model which solves partial differential equations for both the turbulence energy and turbulence dissipation. Converged calculations have been run with both these models. Although, in principle, the more sophisticated turbulence models such as the one- or two-equation models contained in the present code have the potential for being more accurate, they require specification of model constants and model functional forms (e.g., see Ref. 26). As indicated in Ref. 26, most of the currently used models do not appear to show a definitive advantage over mixing length models for general boundary layers developing in arbitrary pressure gradients. The use of such models is currently the focus of work being conducted at SRA.

CURRENT EFFORTS

Objective

Although the Navier-Stokes cascade analysis has shown considerable promise, and given favorable comparisons with data, at the initiation of the present effort successful and efficient utilization of the code required an experienced user. Successful implementation requires the user to exercise two codes; the first being a coordinate generation code and the second being the Navier-Stokes code. The first objective of the present effort was to automate these codes so as to allow a relatively inexperienced user to (i) generate a viable coordinate system and (ii) to obtain accurate solutions with the Navier-Stokes code in an efficient manner. The second objective of the effort was to restructure the Navier-Stokes code so as to obtain converged solutions within 300 seconds of CPU time or less on a modern computer without resorting to code vectorization. Vectorization should allow a further order of magnitude reduction. As shall be demonstrated, both objectives have been met.

Coordinate System

The coordinate system is an important component of the Navier-Stokes analysis. An inappropriate coordinate system may lead to difficulty in obtaining a converged solution and even exhibit physically unrealistic predictions due to geometric truncation error. Therefore, generation of a viable system is mandatory. Any coordinate system used in the analysis should satisfy conditions of (i) generality, (ii) smoothness, (iii) resolvability and (iv) allow easy application of boundary conditions. Obviously, a coordinate system must be sufficiently general to allow application to a wide class of problems of interest if it is to be practical. The metric data associated with the coordinate system must be sufficiently smooth so that the variation from grid point to grid point does not lead to a numerical solution dominated by metric coefficient truncation error; it should be noted that this requirement differs from the requirement of the existence of a specified number of transformation derivatives. The coordinate system must resolve flow regions where rapid flow field changes

occur. Finally, coordinates should allow accurate implementation of boundary conditions; for the cascade this requires that the metric coefficients be continuous across the periodic lines where periodic boundary conditions are to be applied. The coordinate system presently used satisfies all these requirements.

In brief, the coordinate system consists of a set of two families of curves; the $\xi = \text{constant}$ curves such as lines G'G or in Fig. 1 and the $\eta = \text{constant}$ curves such as ABCD or A'ED' in Fig. 1. Under the present effort, the coordinate generation process has been automated and the coordinate construction process is as follows. The coordinate system is constructed by first forming the inner loop A'ED' which includes the blade. This is followed by constructing an outer loop AGBCD which consists of periodic line AB and CD and a frontal curve BC. Both the inner and outer loops are then represented by parametric curves

$$x = x(s), \quad y = y(s) \quad (11)$$

where the parameter varies from zero to unity. The present coordinate generation process utilizes a multi-part transformation for the inner loop. First x and y are expressed as a function of s' , the physical distance along the curve. After normalizing s' such that its range is between zero and unity a local parametrization focuses upon the leading edge region and places $s'' = 0.5$ at the leading edge point where highest resolution is sought. This location must be specified by the user and in general will be in the vicinity of the front stagnation point. This initial transformation is done automatically once the location where maximum resolution is required is specified. Following this first parameterization, s is related to s'' via a hyperbolic tangent parameterization centered about the leading edge point where $s'' = 0.5$.

In this transformation for $s'' < 0.5$

$$s = \frac{1}{2T} \ln \frac{1 + ks''}{1 - ks''} \quad (12a)$$

and for $s'' > 0.5$

$$s = 1 - \frac{1}{2T} \ln \frac{1 + k(1 - s'')}{1 - k(1 - s'')} \quad (12b)$$

where

$$k = 2 \tanh\left(\frac{T}{2}\right) \quad (12c)$$

and the parameter T controls the grid distribution. Increasing T packs points in the vicinity of $s'' = 0.5$

The outer loop is then parameterized so as to relate points on the outer loop to corresponding points on the inner loop. For two points which are periodic, such as G and K in Fig. 2 to maintain periodicity it is necessary that $S_G = 1 - S_K$. This will assure that coordinate points on the upper and lower periodic lines will be periodically aligned.

For points downstream of the five per cent chord location, the inner loop and outer loop points are made to correspond as follows. If G' and K' in Fig. 2 are points on the inner loop aligned with G and K , then

$$S_G = 0.5 S_{G'} + 0.5 (1 - S_{K'}) \quad (13)$$

$$S_K = 1.0 - S_G$$

Downstream of the five per cent chord location, a locally polar parameterization is used as shown in Fig. 3. In this region an origin for the polar coordinates is chosen at $x_0 = 0.05c$ and y_0 halfway between the upper and lower surface locations at the five per cent chord location. The inner loop parameterization s is then tabulated as a function of θ . The outer loop parameterization then follows that given Eq. (13) to relate points P and Q on the outer loop to P' and Q' on the inner loop. Finally, the outer loop parameterization is smoothed in the region between region I ($x/c > .05$) and region II ($x/c < .05$). If N pseudo-radial lines are to be used, the grid points on each loop are chosen at values

$$S_i = (i-1)/(N-1) \quad i = 0, N-1 \quad (14)$$

and points having the same value of s_i on the inner and outer loops define the end points for a given pseudo-radial line (e.g. G'G of Fig. 2). Since the loops are parameterized so that s varies rapidly in the region of the leading edge, this process effectively packs points into the leading edge region about the location where $s = 0.5$.

Following the construction and parameterization of the inner and outer loop, two intermediate loops are constructed as shown in Fig. 4. The first intermediate loop is constructed downstream of $x/c = 0.05$ a given vertical distance, h_1 , from the inner loop. Upstream of $x/c = 0.05$, the distance is measured along a pseudo-radial line as shown in Fig. 4. A similar loop is constructed inside the outer loop with the vertical distance being maintained to the end of the periodic region, points R and S. The inner secondary loop is parameterized to correspond to the primary loop points it is connected with via the vertical or pseudo-radial lines; i.e.,

$$S_{S'} = S_S$$

Similarly,

$$S_{T'} = S_T$$

These four parameterized loops allow the construction of the pseudo-radial lines such as G'G of Fig. 2 via the multi-loop method originally developed by Eiseman (Ref. 27).

The multi-loop method requires introduction of a position vector $\vec{P}(r,s)$ with components (x,y) which will represent the coordinate location of grid points. Based upon the four loop construction process, vectors $\vec{P}_i(s)$ are defined with $i = 1,2,3,4$. Each \vec{P}_i has coordinate (x_i,y_i) associated with it at specific values of s through the previously described construction process. A radial parameter, r , is then introduced. This parameter is defined at the downstream boundary, see Fig. 4, as the distance from the loop in question to the inner loop normalized by the distance from the outer loop to the inner loop. Thus, $r_1 = 0$, $r_2 = h_1/h_3$, $r_3 = (h_3 - h_2)/h_3$, $r_4 = 1$. With the definition of these quantities the general position vector $\vec{P}(r,s)$ is related to the loop position vectors $\vec{P}_1(s)$, $\vec{P}_2(s)$, $\vec{P}_3(s)$ and $\vec{P}_4(s)$ via

$$\begin{aligned} \vec{P}(r,s) = & (1-r)^2(1-a_1r)\vec{P}_1(s) + (a_1+2)(1-r)^2r\vec{P}_2(s) \\ & + r^2[1-a_2(1-r)]\vec{P}_4(s) + (a_2+2)r^2(1-r)\vec{P}_3(s) \end{aligned} \quad (15)$$

where

$$\begin{aligned} a_1 &= \frac{2}{3r_2 - 1} \\ a_2 &= \frac{2}{3(1 - r_2) - 1} \end{aligned} \quad (16)$$

it should be noted that at $r = 0$, $\vec{P}(0, s) = \vec{P}_1(s)$ and at $r = 1$, $\vec{P}(1, s) = \vec{P}_4(s)$. Further since at $r = 0$,

$$\frac{\partial P}{\partial r}(0, s) = [\vec{P}_2(s) - \vec{P}_1(s)](a_1 + 2) \quad (17)$$

and at $r = 1$

$$\frac{\partial P}{\partial r}(1, s) = [\vec{P}_4(s) - \vec{P}_3(s)](a_2 + 2) \quad (18)$$

specification of the derivatives at the inner and outer boundaries is determined by the parametric representation of intermediate loops 2 and 3. Thus the four loop method allows specification of the boundary point locations and coordinate angles at these boundaries.

After loops 2 and 3 are parameterized to satisfy the coordinate angle at the boundary points, the grid is constructed as follows. If the grid is to contain M pseudo-radial lines (such as line $G'C$ of Fig. 1) and N pseudo-azimuthal lines (such as line JLM), the values of the pseudo-radial coordinate are

$$r(i) = i/(N-1) \quad i = 0, 1, 2, \dots, N-1$$

and the values of the pseudo-azimuthal coordinate are

$$s(j) = j/(M-1) \quad j = 0, 1, 2, \dots, M-1$$

Then the position vector; i.e., the grid locations x, y for each point in the grid is given by Eq. (15).

The preceding has assumed a uniform spacing in the radial direction. If radial grid point concentration is desired, it is simply necessary to assume a radial distribution function. The present analysis assumed a distribution function

$$R = \left[1 - \frac{\tanh D(1-r)}{\tanh D} \right] \quad (19)$$

which concentrates points in the wall region. Grid points are then chosen at $r(i) = (i)/(N-1)$ and the analysis proceeded as outlined.

The input required for the grid construction process is as follows:

1. Number of pseudo-radial points
2. Number of pseudo-azimuthal points
3. Vertical distance from branch cut to periodic line, h_3
(See Fig. 4)
4. Angle of branch cut line, θ_2 - This is zero in Fig. 4
5. Angle of leading edge line, θ_3
6. Approximate leading edge radius of blade - This sets the pseudo-azimuthal spacing in the leading edge
7. Reference flow Reynolds number based on free stream conditions and blade chord - This sets normal grid spacing in the vicinity of the wall
8. Data points or functional form to define the blade shape

Grids generated with this procedure are shown in Figs. 5 and 6. Fig. 5 represents a compressor cascade corresponding to the cascade of Hobbs, et al (Ref. 14). This cascade was used in the ensuing calculations which demonstrate the increase in efficiency of the Navier-Stokes code obtained under this effort. The second cascade which is shown in Fig. 6 corresponds to the turbine cascade of Turner (Ref. 11). Both coordinate systems were generated from the input given in items 1-8 above and had the required properties in terms of grid smoothness and resolution to be viable coordinate systems.

The automated procedure developed to date is confined to 'C' grids such as those shown in Figs. 5 and 6. Recently SRA has developed an 'O' grid generator (Ref. 16) and although this procedure currently requires considerable user interaction to obtain a viable grid, automation of the 'O' grid generator should be straightforward based upon the techniques developed under the present effort.

Navier-Stokes Analysis

Having generated a viable coordinate system, the second step in the process is to obtain a solution of the Navier-Stokes equations for the specified coordinate system and desired flow conditions. Although the deck has proven capable of obtaining accurate solutions for a variety of cascade configurations and flow conditions (e.g. Refs. 4, 5, 8, 9, 16), successful operation had required an experienced user. Furthermore, although computer run times were promising, they obviously could be improved, therefore, two subtasks were undertaken in the present effort. These were (i) decrease of run time and (ii) automation of input/output.

In regard to the first item, decrease in run time, the original cascade code was actually a general code which could be used to solve a wide variety of problems with little if any code revision required by the user. Although this generality represents a major advantage in a general research code, it does exact a price in terms of run time. Under a previous effort some of the options originally available in the general code which were not required for the cascade problem were removed to create a specific cascade version of the deck. These items included features such as a polar coordinate option, a two-phase and reacting flow option, etc. Under the present effort this work was continued to further decrease run time.

Among the items performed were creation of specific tridiagonal block matrix inversion routines for systems of three equations and three unknowns, incorporation of small subroutines within the calling routines and extensive recoding of frequently called subroutines to eliminate small "DO LOOPS". These modifications have not changed the flexibility or generality of the code; i.e., they are transparent to the user and have reduced run time by a factor slightly greater than two. In its current state, the code solves the continuity and two momenta equations for turbulent flow in approximately

0.00118 secs per time step per grid point on a CRAY-1 computer. Although an energy equation can be solved on request by user, the necessary fast 4×4 matrix inverters have not yet been written and, therefore, at present general inversion routines must be used. However, inclusion of specific 4×4 matrix inverters is a straight-forward if somewhat tedious task which could easily be part of a future effort. It should be noted that the code is not vectorized and careful vectorization would be expected to decrease run time by a factor of ten. In regard to run time per case, successful calculations have been made using a grid of 113×30 points. Such a grid requires approximately 4 secs per time step with a potential of 0.4 secs per time step if code vectorization were performed. The question of the run time per case then rests on the number of time steps to convergence.

Although the cascade Navier-Stokes analysis can be used both for time-dependent and steady-state flow situations, and although good results for time-dependent flows have been obtained with an airfoil version of this code (Ref. 28), the focus of the present investigation is flows whose steady solution is sought. In such a case, it is not necessary to accurately follow the transient motion and indeed it may be advantageous not to follow the transient motion accurately, if this accelerates convergence to steady state. The present approach is based upon this concept and utilizes the matrix conditioning technique of Refs. 29 and 30 to accelerate convergence to a steady state.

Using the techniques described in Refs. 29 and 30 has allowed cascade calculations to converge very rapidly even for low Mach number subsonic flows which in general can be difficult to converge. A typical convergence history is presented in Fig. 7 which presents residual versus time step number for the subsonic cascade calculation corresponding to the experiment of Hobbs, et al (Ref. 14). As can be seen, the maximum residual in the flow field drops by three and one-half orders of magnitude in seventy time steps. The reason for the sudden jump at time sixty will be discussed shortly. The maximum residual is defined by the maximum imbalance of any equation at any point when the time-derivative terms are omitted. At seventy time steps the solution has essentially stopped changing and as will be shown, the surface pressure calculated is in very good agreement with that measured. At 4 secs

CRAY CPU time per time step the present calculation can be considered converged in less than 300 CPU system secs.

The reason for the sudden jump in residual at time step 60 is due to the method in which the calculation was run. The calculation was initiated with artificial dissipation parameters, d_x and d_y , equal to 0.5 (see the section on artificial dissipation). At time step sixty this was reduced to 0.05 except in the immediate vicinity of the leading edge $x/c < .02$ where it was kept at 0.5 due to marginal resolution in this region.

A comparison between the calculated and measured surface pressure for this case is shown in Fig. 8. As can be seen, the calculated and measured values are in excellent agreement. Calculated velocity and pressure coefficient contours are shown in Figs. 9-11, and a velocity vector plot is shown in Fig. 12.

The second Navier-Stokes subtask considered under the present effort concerns code input. Under the present effort many of the items previously required to run a case have been automatically set thus allowing a new user to run the code. With the current cascade code once the grid has been generated only the following items are required to run the code:

- 1 - Restart flag
- 2 - Number of grid points in each direction
- 3 - Upstream flow angle, upstream total pressure, downstream static pressure
- 4 - Reference velocity, temperature density and viscosity to set reference Reynolds and Mach number
- 5 - Artificial viscosity
- 6 - Number of time steps requested

ESTIMATES OF TECHNICAL FEASIBILITY

Under the present effort, an existing coordinate generator/Navier-Stokes solver has been automated and streamlined so as to allow a new user to obtain accurate cascade solutions in an efficient manner. The coordinate generator requires relatively little input other than blade shape and spacing input and has been used to generate two very different cascade coordinate systems. Further effort of this type for the 'O' grid generator would lead to a robust, easily used cascade coordinate generation code for both 'O' and 'C' grid types.

The second general item investigated focused upon the Navier-Stokes code. The work done under the present effort has allowed steady cascade flow fields to be generated in less than 300 secs of CRAY CPU time without resorting to code vectorization. At commercial computer rates this represents a very practical cost. Although code vectorization would be a time-consuming procedure, it is straight-forward and it is estimated that a vectorized code could obtain solutions in 30 secs of CRAY CPU time. This vectorized run time would reduce costs to the point where multiple runs on a daily basis could be considered if so desired thus allowing the Navier-Stokes code to be a practical design tool. Extension of the current rapid run time version to include an energy equation would be a straight-forward task. In this regard it should be re-emphasized that the current code does include an energy equation (although not optimized) and has been successfully used in heat transfer calculations (Ref. 16).

The present effort has concentrated upon steady flow fields at very low subsonic through transonic Mach numbers, although the code solves the time-dependent equations and could be used for time-dependent problems. Results obtained for flow about an isolated airfoil oscillating through a dynamic stall loop have been very encouraging in verifying the time-accuracy of the procedure for free stream Mach numbers at or above 0.30 (Ref. 28). It should be recalled that for steady flows converged solutions can be obtained easily for much lower free stream Mach numbers, however, the technique used is not time-accurate. Current efforts at SRA are aimed at modifying the algorithm to allow time-accurate calculations for low free stream Mach numbers.

Since many time-dependent problems require small physical steps, many time steps may be required to model a time-dependent process. In these cases, a fast vectorized code would obviously be a major advantage. Once such a code was available, it would be practical to apply the code to problems such as unsteady flow in cascades due to blade wake passing and flows with back pressure or inlet perturbations on a routine basis. The code could also be used in a full nonlinear approach to the rotating stall problem.

REFERENCES

1. Farrel, C. and Adameczyk, J.: Full Potential Solution of Transonic Quasi-3-D Flow Through a Cascade Using Artificial Compressibility. ASME Paper 81-GT-70, 1981.
2. Casper, J.R., Hobbs, D.E. and Davis, R.L.: The Calculation of Two-Dimensional Compressible Potential Flow in Cascades Using Finite Area Techniques. AIAA Paper 79-007, 1977.
3. Hansen, E.C., Serovy, G.K. and Sockol, P.M.: Axial Flow Compressor Turning Angle and Loss by Inviscid-Viscous Interaction Blade-to-Blade Computation, Journal of Engineering for Power, Vol. 102, 1980.
4. Shamroth, S.J. and McDonald, H.: An Assessment of an Ensemble-Averaged Navier-Stokes Calculation Procedure for Cascade Flow Fields. Scientific Research Associates Report R82-920011-F, 1982.
5. Shamroth, S.J. McDonald, H. and Briley, W.R.: Prediction of Cascade Flow Fields Using the Averaged Navier-Stokes Equations. To be published in ASME Journal of Engineering for Power.
6. Rehyner, T. and Flugge-Lotz, I.: The Interaction of Shock Waves with a Laminar Boundary Layer. International Journal of Nonlinear Mechanics, Vol. 3 1968.
7. Shamroth, S.J., Gibeling, H.J. and McDonald, H.: A Navier-Stokes Solution of Laminar and Turbulent Flow Through a Cascade of Airfoils. AIAA Paper No. 80-1426, 1980. (Also, SRA Report R79-920004-F, 1982.)
8. Shamroth, S.J., McDonald, H. and Briley, W.R.: A Navier-Stokes Solution for Transonic Flow Through a Cascade. SRA Report R82-920007-F, 1982.
9. Shamroth, S.J., McDonald, H. and Briley, W.R.: Application of a Navier-Stokes Analysis to Transonic Cascade Flow Fields. ASME Paper 82-GT-235, 1982.
10. McDonald, H., Shamroth, S.J. and Briley, W.R.: Transonic Flows with Viscous Effects, Transonic Shock and Multi-Dimensional Flows: Advances in Scientific Computing. Academic Press, New York, 1982.
11. Turner, A.B.: Local Heat Transfer Measurements on a Gas Turbine Blade. Journal of Mechanical Engineering Sciences, Vol. 13, 1971.
12. Hylton, L.D., Mihelc, M.S., Turner, E.R., Nealy, D.A. and York, R.E.: Analytical and Experimental Evaluation of the Heat Transfer Distribution Over the Surface of Turbine Vanes. NASA-CR-168015, May 1983.
13. Stephens, H.E. and Hobbs, D.E.: Design and Performance of Supercritical Airfoils for Axial Flow Compressors. Pratt and Whitney Aircraft Report PR11455, 1979.

REFERENCES (Continued)

14. Hobbs, D.E., Wagner, J.H., Dannenhoffer, J.F., Dring, R.P.: Wake Experiment and Modelling for Fore and Aft-loaded Compressor Cascade. Pratt and Whitney Aircraft Report FR13514, 1980.
15. Dring,, R.P., Joslyn, H.D. and Hardin, L.W.: An Investigation of Axial Compressor Rotor Aerodynamics. ASME Journal of Engineering for Power, Vol. 104, 1982.
16. Yang, R.-J., Weinberg, B.C., Shamroth, S.J. and McDonald, H.: SRA Report 310003-10, 1984.
17. Shamroth, S.J., Yang, R.-J. and McDonald, H.: SRA Report 920015-F, 1984.
18. Briley, W.R. and McDonald, H.: Solution of the Multi-Dimensional Compressible Navier-Stokes Equations by a Generalized Implicit Method. Journal of Computational Physics, Vol. 24, 1977.
19. Lindemuth, I. and Killeen, J.: Alternating Direction Implicit Techniques for Two-Dimensional Magnetohydrodynamic Calculations. Journal of Computational Physics, 13, 1973.
20. Briley, W.R. and McDonald, H.: On the Structure and Use of Linearized Block Implicit Schemes. Journal of Computational Physics, Vol. 34, 1980.
21. Douglas, J. and Gunn, J.E.: A General Formulation of Alternating Direction Methods. Numerische Math., Vol. 6, 1964, pp. 428-453.
22. Briley, W.R., Buggeln, R.C. and McDonald, H.: Computation of Laminar and Turbulent Flow in 90 Degree Square Duct and Pipe Bends Using the Navier-Stokes Equations. SRA Report R82-920009-F, 1982.
23. Liu, N.S., Shamroth, S.J. and McDonald, H.: Numerical Solution of the Navier-Stokes Equations for Compressible Turbulent Two/Three Dimensional Flows in the Terminal Shock Region of an Inlet/Diffuser. AIAA Paper 83-1892, 1983.
24. Briley, W.R. and McDonald, H.: Computation of Three-Dimensional Horseshoe Vortex Flow Using the Navier-Stokes Equations. Seventh International Conference on Numerical Methods in Fluid Dynamics, 1980.
25. Schlichting, H.: Boundary Layer Theory, McGraw Hill, New York, 1960.
26. Patel, V.C., Rodi, W. and Scheurer, G.: Evaluation of Turbulence Models for Near Wall and Low Reynolds Number Flows. Third Symposium on Turbulence Shear Flows. University of California, Davis, 1981.

REFERENCES (Continued)

27. Eiseman, P.R.: Coordinate Generation with Precise Controls over Mesh Properties. *Journal of Computational Physics*, Vol. 47, 1982.
28. Shamroth, S.J.: Calculation of Steady and Oscillating Airfoil Flow Fields via the Navier-Stokes Equations. *AIAA Paper 84-525*, 1984.
29. Briley, W.R., McDonald, H. and Shamroth, S.J.: A Low Mach Number Euler Formulation and Application to Time Iterative LBI Schemes. *AIAA Journal*, Vol. 21, 1983.
30. Briley, W.R. and McDonald, H.: Computational Fluid Dynamic Aspects of Internal Flow. *AIAA Paper 79-1455*, 1979.

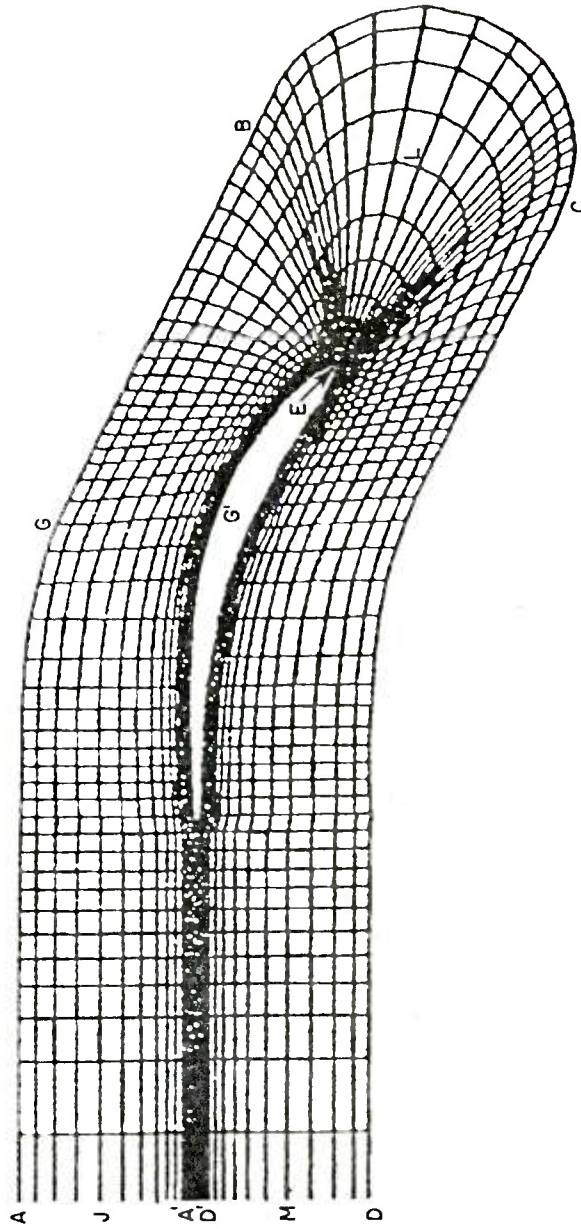


Fig. 1 - Constructive coordinate system.

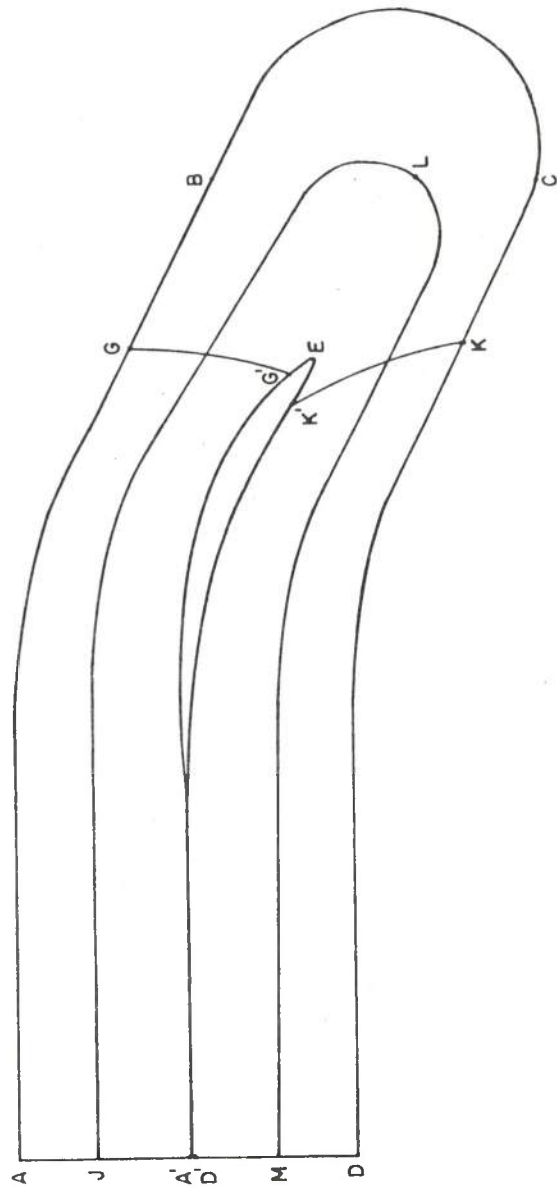


Fig. 2 - Constructive coordinate system - outer loop parameterization.

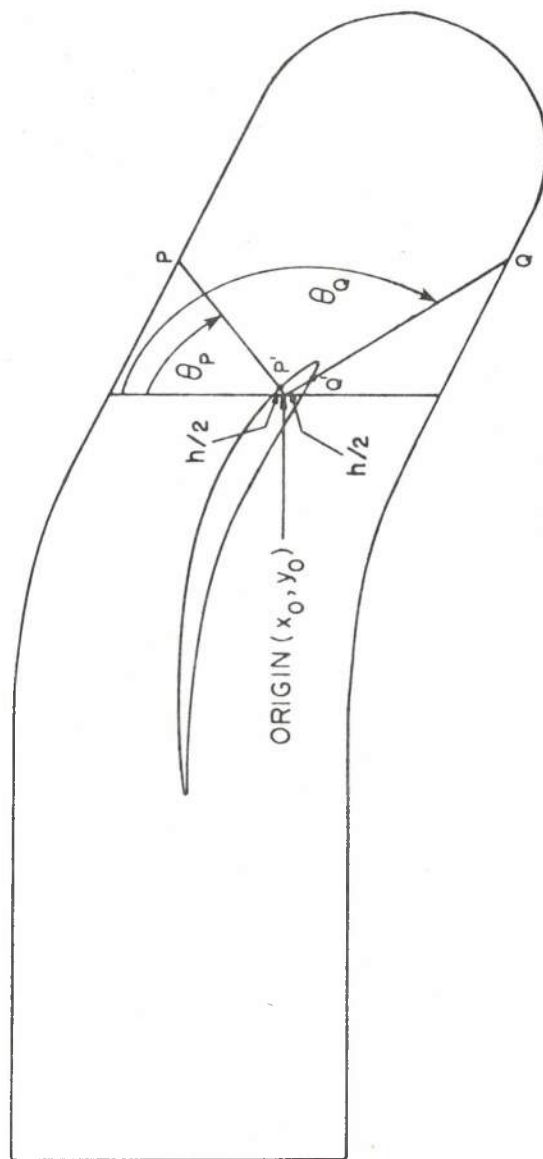


Fig. 3 - Constructive coordinate system - leading edge outer loop parameterization.

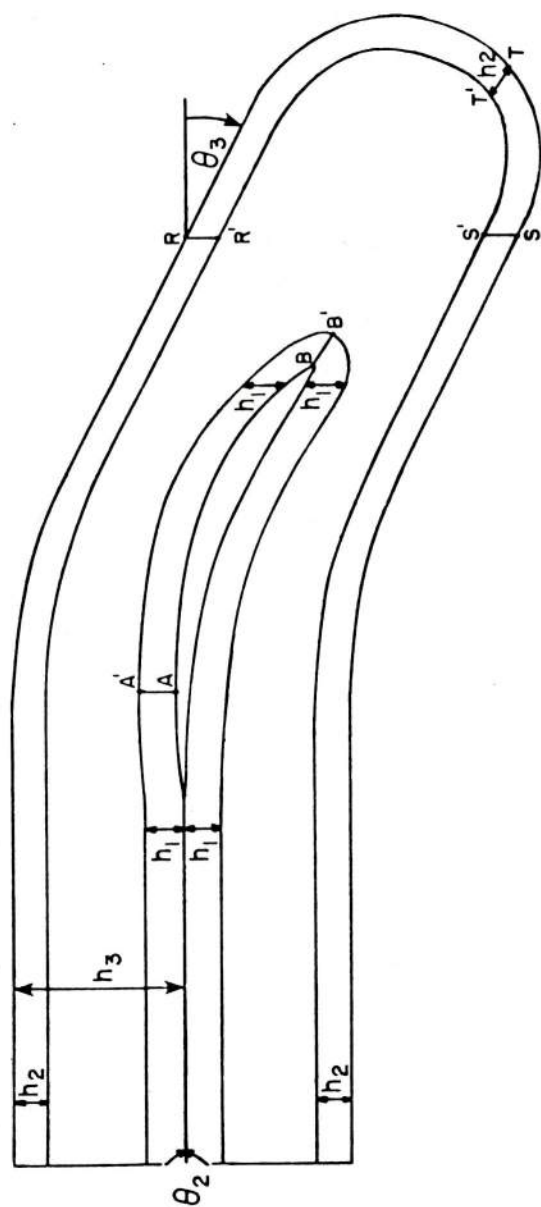


Fig. 4 - Constructive coordinate system - secondary loops.

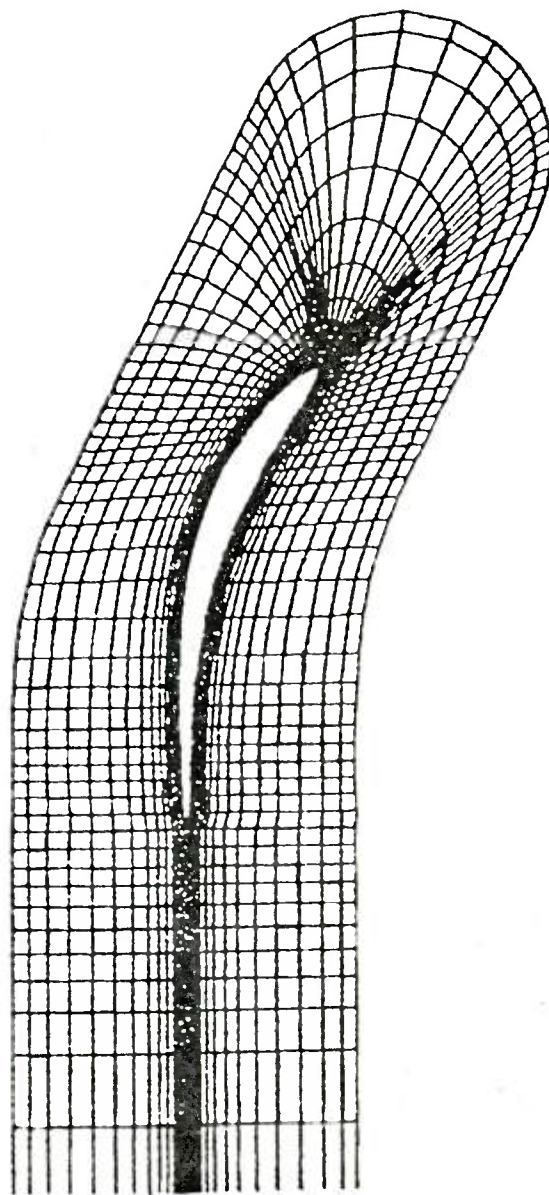


Fig. 5 - Coordinate system for Hobbs cascade.

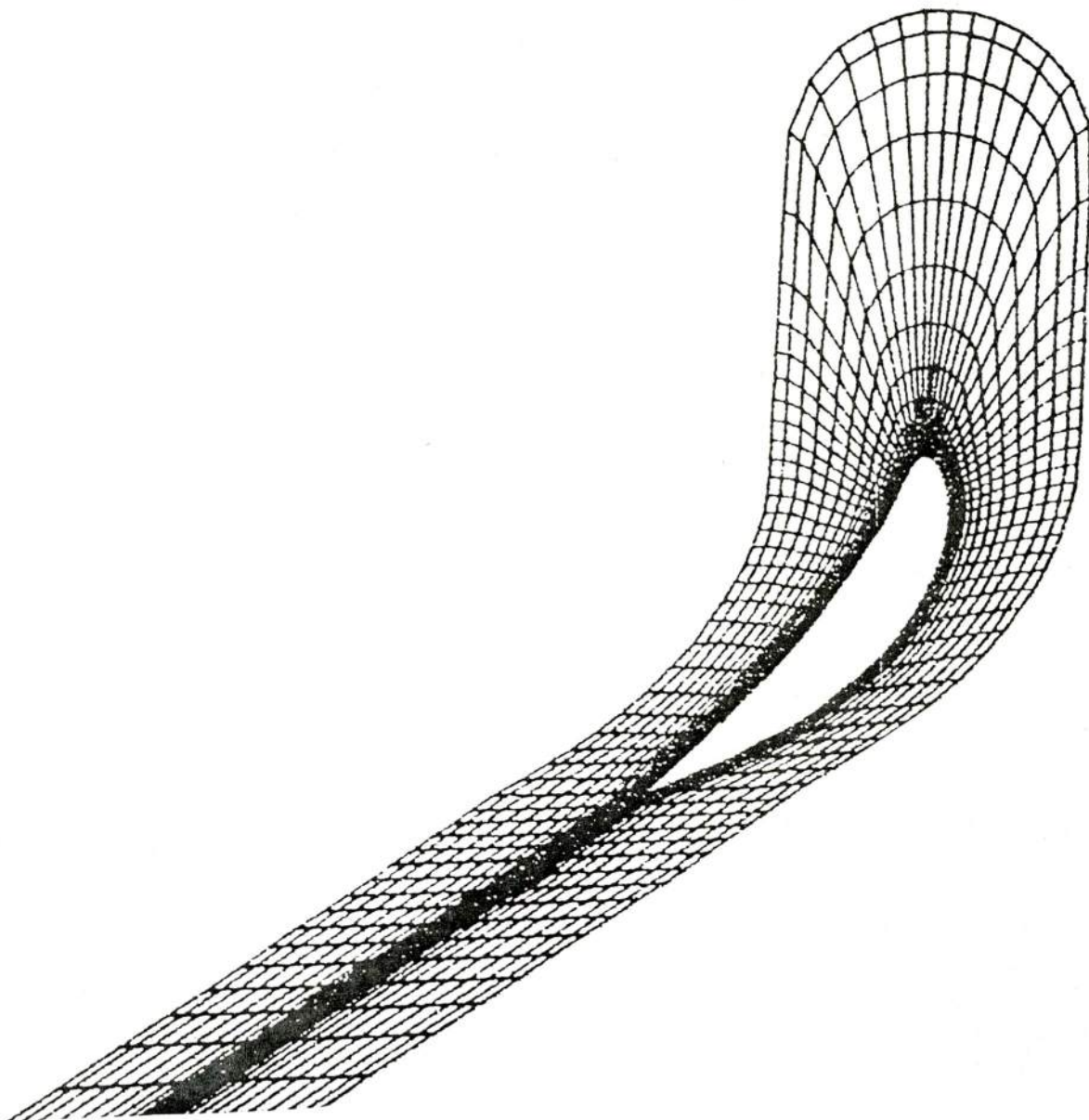


Fig. 6 - Coordinate system for Turner cascade.

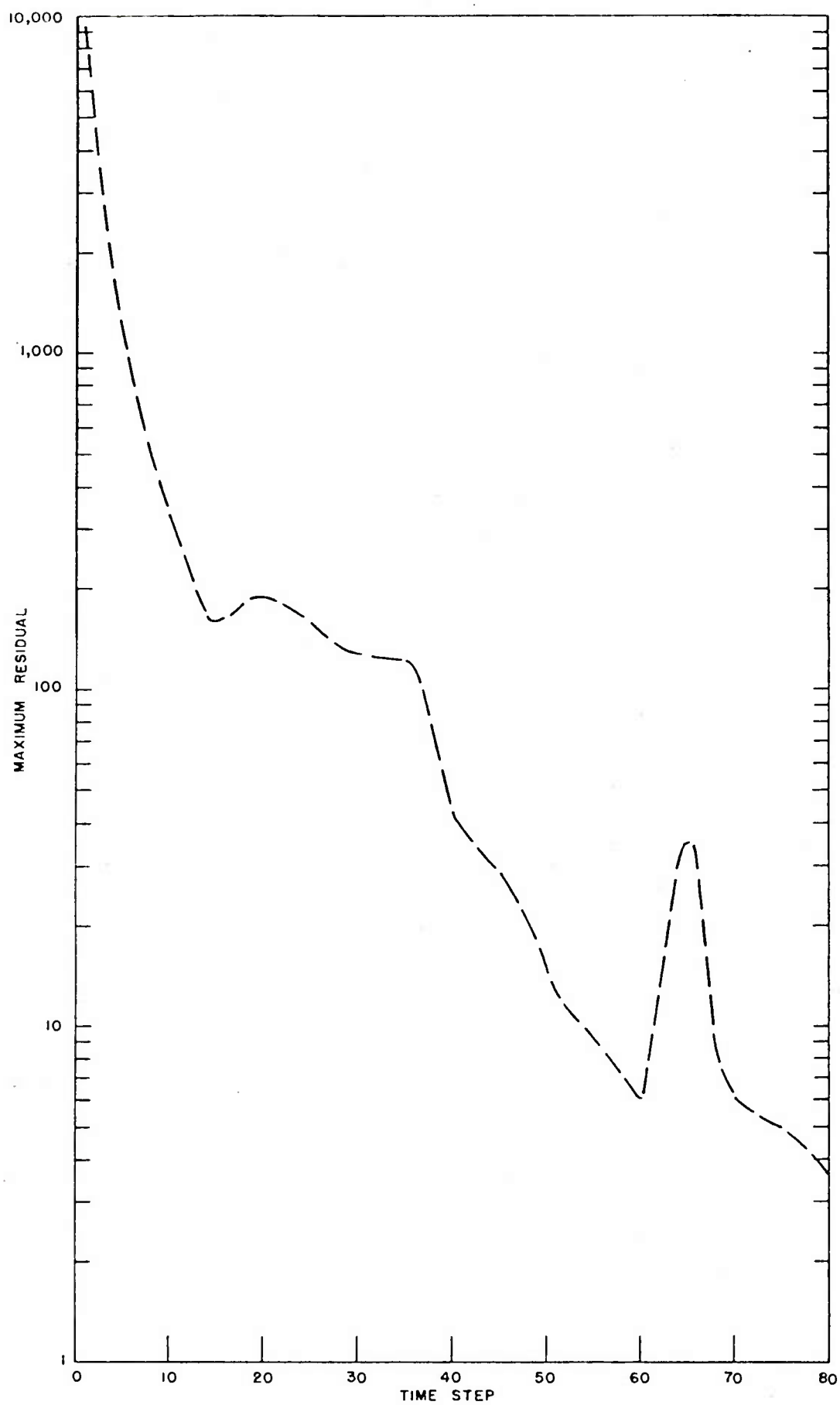


Fig. 7 - Iteration history, Hobbs subsonic cascade.

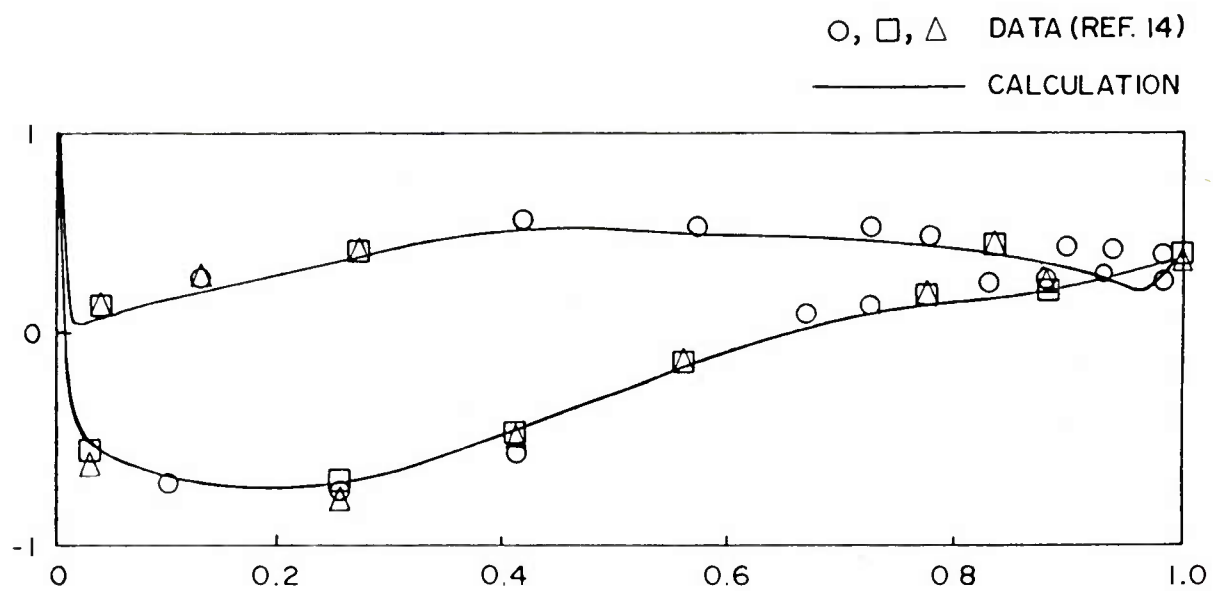


Fig. 8 - Calculated and measured pressure distribution,
subsonic compressor cascade.

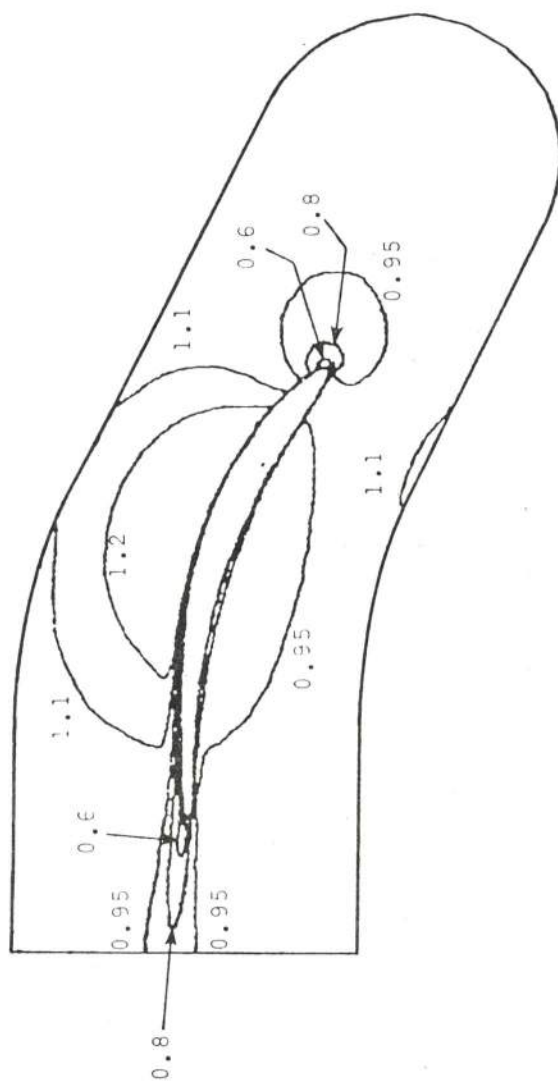


Fig. 9 - U-velocity contours for Hobbs cascade.

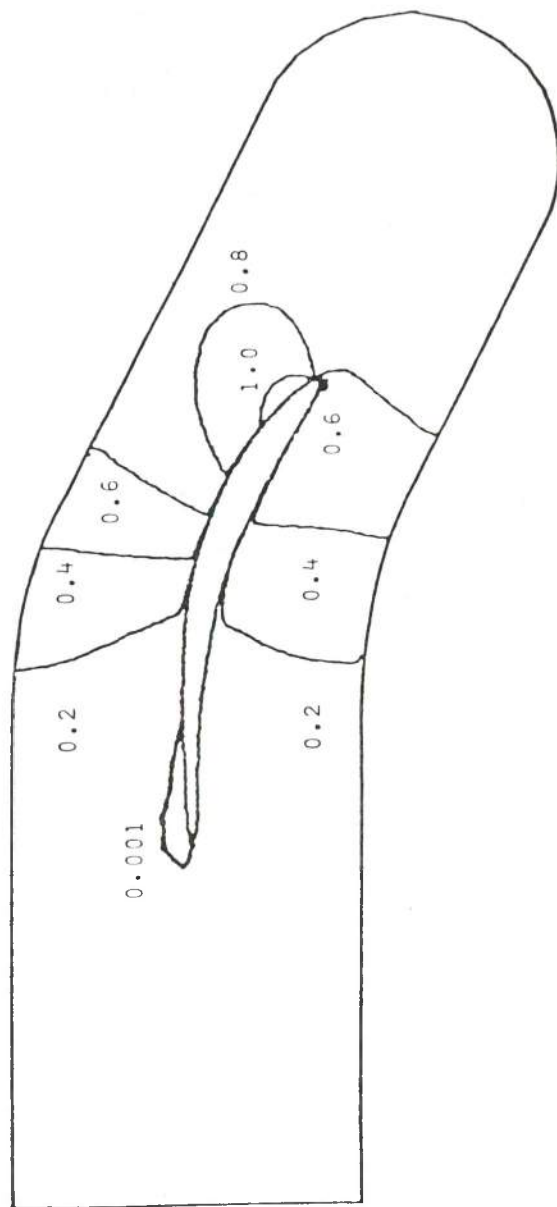


Fig. 10 - W-velocity contours for Hobbs cascade.

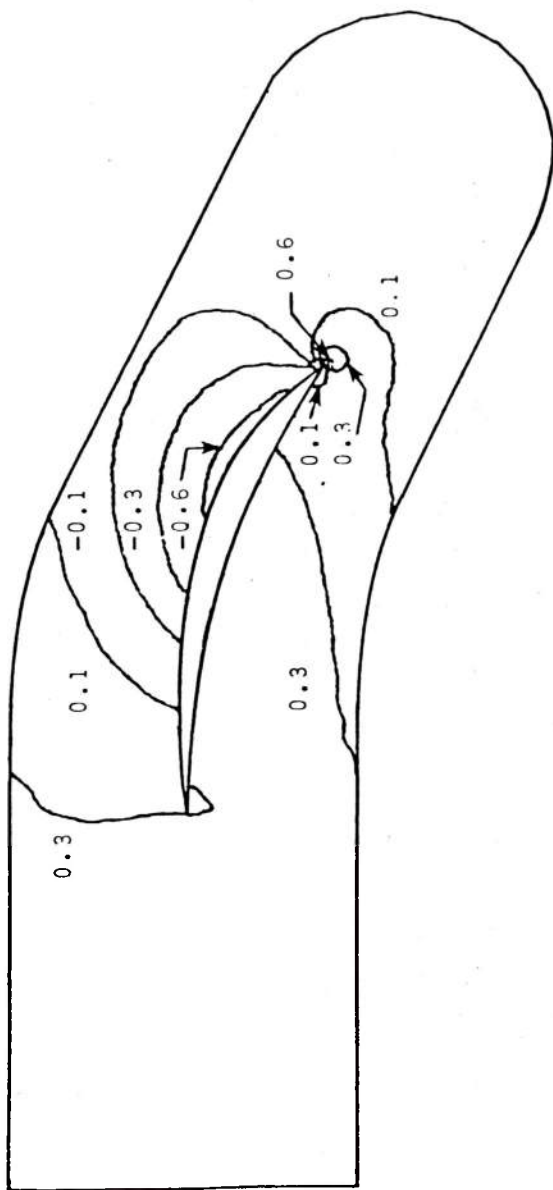


Fig. 11 - Pressure coefficient contours for Hobbs cascade.

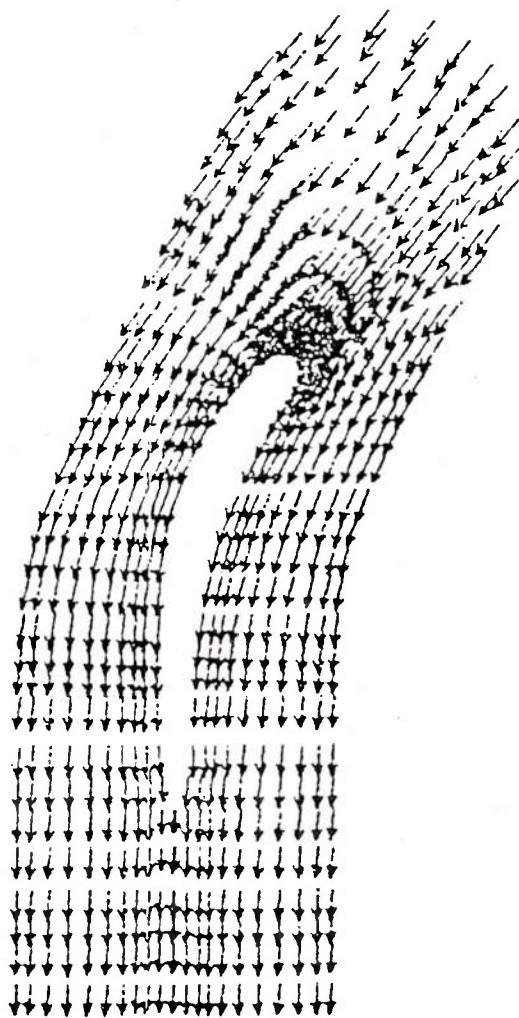


Fig. 12 - Velocity vector plot for Hobbs cascade.

APPENDIX A - Split LBI Algorithm

Linearization and Time Differencing

The system of governing equations can be written as a single grid point in the following form:

$$\partial H(\phi)/\partial t = D(\phi) + S(\phi) \quad (\text{A-1})$$

where ϕ is the column-vector of dependent variables, H and S are column-vector algebraic functions of ϕ , and D is a column vector whose elements are the spatial differential operators which generate all spatial derivatives appearing in the governing equation associated with that element.

The solution procedure is based on the following two-level implicit time-difference approximations of (A-1):

$$(H^{n+1} - H^n)/\Delta t = \beta(D^{n+1} + S^{n+1}) + (1-\beta)(D^n + S^n) \quad (\text{A-2})$$

where, for example, H^{n+1} denotes $H(\phi^{n+1})$ and $\Delta t = t^{n+1} - t^n$. The parameter β ($0.5 \leq \beta \leq 1$) permits a variable time-centering of the scheme, with a truncation error of order $[\Delta t^2, (\beta - 1/2) \Delta t]$.

A local time linearization (Taylor expansion about ϕ^n) of requisite formal accuracy is introduced, and this serves to define a linear differential operator L such that

$$D^{n+1} = D^n + L^n (\phi^{n+1} - \phi^n) + O(\Delta t^2) \quad (\text{A-3})$$

Similarly,

$$H^{n+1} = H^n + (\partial H/\partial \phi)^n (\phi^{n+1} - \phi^n) + O(\Delta t^2) \quad (\text{A-4})$$

$$S^{n+1} = S^n + (\partial S/\partial \phi)^n (\phi^{n+1} - \phi^n) + O(\Delta t^2) \quad (\text{A-5})$$

Equations (A-3,4,5,) are inserted into Eq. (A-2) to obtain the following system which is linear in ϕ^{n+1}

$$(A - \beta \Delta t L^n) (\phi^{n+1} - \phi^n) = \Delta t (D^n + S^n) \quad (\text{A-6})$$

and which is termed a linearized block implicit (LBI) scheme. Here, A denotes a square matrix defined by

$$A \equiv (\partial H/\partial \phi)^n - \beta \Delta t (\partial S/\partial \phi)^n \quad (\text{A-7})$$

Special Treatment of Diffusive Terms

The time differencing of diffusive terms is modified to accomodate cross-derivative terms and also turbulent viscosity and artificial dissipation coefficients (i.e., ν_e , d_i) which depend on the solution variables.

These diffusive coefficients are evaluated explicitly at t^n during each time step. Notationally, this is equivalent to neglecting terms proportional to $\partial \nu_e / \partial \phi$ or $\partial d_j / \partial \phi$ in L^n , which are formally present in the Taylor expansion (A-3), but retaining all terms proportional to ν_t or d_j in both L^n and D^n .

In addition, the viscous terms in the present formulation include a number of spatial cross-derivative terms which are evaluated explicitly at t^n . To preserve notational simplicity, it is understood that all cross-derivative terms appearing in L^n are neglected but are retained in D^n .

Consistent Splitting of the LBI Scheme

To obtain an efficient algorithm, the linearized system (A-6) is split using ADI techniques. To obtain the split scheme, the multidimensional operator L is rewritten as the sum of three "one-dimensional" sub-operators L_i ($i = 1, 2, 3$) each of which contains all terms having derivatives with respect to the i -th spatial coordinate. The split form of Eq. (A-6) can be derived either by following the procedure described by Douglas and Gunn in their generalization and unification of scalar ADI schemes, or using approximate factorization. In either case, for the present system of equations the split algorithm is given by

$$(A - \beta \Delta t L_1^n) (\phi^* - \phi^n) = \Delta t (D^n + S^n) \quad (A-8a)$$

$$(A - \beta \Delta t L_2^n) (\phi^{**} - \phi^n) = A (\phi^* - \phi^n) \quad (A-8b)$$

$$(A - \beta \Delta t L_3^n) (\phi^{n+1} - \phi^n) = A (\phi^{**} - \phi^n) \quad (A-8c)$$

where ϕ^* and ϕ^{**} are consistent intermediate solutions [18,20]. If spatial derivatives appearing in L_i and D are replaced by three-point difference formulas, then each step in Eqs. (A-8a, b, c) can be solved by a block-tridiagonal elimination.